Two-Dimensional Images of CF_2 Density in CF_4/Ar Plasmas by Laser-Induced Fluorescence in a GEC RF Reference Cell

Brian K. McMillin and Michael R. Zachariah

***Abstract*— Spatially resolved two-dimensional (2-D) maps of the relative CF_2 density in low-pressure CF_4/Ar RF discharges, generated within a parallel-plate gaseous electronics conference (GEC) reference reactor, have been obtained using planar laser-induced fluorescence imaging (PLIF). The results illustrate the changes in CF_2 density and distribution in the central plane of the discharge region as flowrate is varied over 10–100 sccm at constant power and pressure, and as pressure is varied over 13.3–133.3 Pa at constant flowrate and power.**

PLANAR laser-induced fluorescence (PLIF) imaging was used to map the spatially resolved time-averaged CF_2 density distribution in low-pressure RF CF_4/Ar etching plasmas. The discharges examined here, as in our previous studies [1], were generated within a capacitively coupled parallel-plate asymmetrically driven gaseous electronics conference (GEC) reference cell. The objective of this work was to obtain two-dimensional (2-D) concentration maps of the CF_2 radical over a range of conditions for benchmarking and verification of plasma chemistry models. In fluorocarbon etching plasmas, which are widely used in microelectronics integrated circuit manufacturing, the CF_2 radical is an important species because it influences the balance between polymer deposition and etching of silicon and silicon dioxide [2]. Additional details and results of these experiments are available elsewhere [3] and will be discussed in a future publication.

In this investigation, a thin sheet (5×25 mm) of quadrupled Nd:YAG laser light (266 nm) was used to illuminate the central vertical plane of the discharge, and thereby excite transitions in the $A(0, 2, 0) \leftarrow X(0, 1, 0)$ band of CF_2. The resulting broadband fluorescence over 300–400 nm was imaged at a 90° angle to the illumination plane with an intensifier-gated cooled charge-coupled device (CCD) camera using an f/4.5 ultraviolet (UV) lens. The spatial resolution of these measurements was determined by the laser sheet thickness of ~5 mm and the imaged dimensions of the camera pixels in the object plane ($\sim 0.2 \times 0.2$ mm). Note that these measurements, therefore, are not line-of-sight integrated through the discharge.

To relate the signal in the raw fluorescence images to the relative CF_2 number density [CF_2], the plasma emission was first subtracted and then the images were normalized for spatial variations in laser energy and detector response. No corrections for fluorescence yield were necessary here because no significant differences in the fluorescence decay times were observed for the conditions examined [3]. Although the absolute CF_2 density was not determined in this study, investigators using a GEC cell recently reported [4] CF_2 densities of $\sim 10^{12}$–10^{13} cm^{-3} in CF_4/CHF_3 plasmas at similar conditions.

Fig. 1(a)–(c) shows images which illustrate the changes in the [CF_2] distribution as flowrate is varied, while Fig. 1(d)–(f) illustrates the effect of varying pressure. In all cases, the feed gas is introduced through a showerhead arrangement of holes in the upper electrode, and exits radially and symmetrically from the discharge region. In each image, the [CF_2] is shown in a rainbow false color map, where violet and red indicate low and high density, respectively. The powered (lower) and grounded (upper) electrodes are shown in black. The imaged region includes approximately one-half of the discharge, extending from the axial centerline to ~1 cm beyond the edge of the electrodes.

Generally speaking, large radial variations in [CF_2] are observed, with the peak occurring at $r \sim 3$–5 cm. This is presumably due to an enhanced electric field near the edge of the powered electrode, which leads to increased excitation and dissociation there. Over much of the central region of the discharge, the axial distribution of CF_2 is relatively symmetric, with the peak occurring near the center of the electrode gap. Increasing the flowrate [Fig. 1(a)–(c)] at constant power and pressure resulted in significant changes in the [CF_2], and modest changes in its distribution as well. In general, the [CF_2] increases with flowrate up to ~18 sccm, while the spatial distribution remains essentially unchanged. Further increases in flowrate, however, lead to a decrease in the overall [CF_2], and an enhancement of the [CF_2] near the edge of the electrodes with respect to the center of the discharge (i.e., $r = 0$). Because the CF_2 production rate likely remains constant for these cases, the observed changes in the overall [CF_2] suggest a competition among its various loss processes [3], which include convection, gas–phase recombination, surface losses, and diffusion.

While further research is necessary to be certain, this variation in [CF_2] might be explained as follows. At moderately high flowrates (i.e., 25 sccm), further increases in the flowrate yield a decrease in the accumulation of CF_2 within the discharge because the dissociation products are convected away more rapidly. As the flowrate is reduced (from say, 50 sccm), initially the [CF_2] increases because of reduced convective losses. Although the CF_2 gas–phase recombination (i.e., $CF_2 + F + M \rightarrow CF_3 + M$) [5] may be somewhat more important at lower flowrates, it cannot explain the observed decrease in [CF_2] at very low flows because this recombination

Manuscript received June 20, 1995; revised October 3, 1995.

B. K. McMillin is with the Lam Research Corporation, Fremont, CA 94538 USA.

M. R. Zachariah is with the Chemical Science and Technology Laboratory, the National Institute of Standards and Technology, Gaithersburg, MD 20899 USA.

Publisher Item Identifier S 0093-3813(96)02178-9.

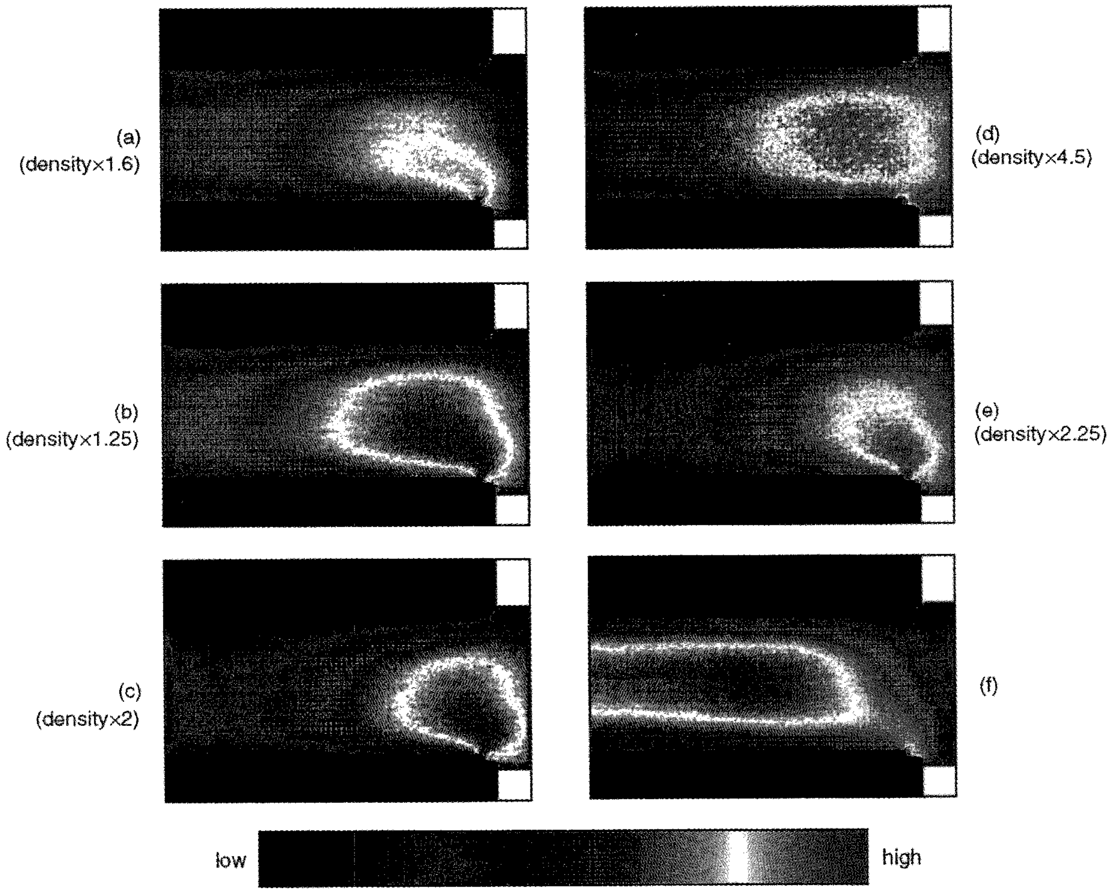

Fig. 1. PLIF images (a)–(c) show the effect of varying flowrate on the spatially resolved CF_2 relative density distribution in the central plane of 25% CF_4/Ar RF discharges at 20 W, 66.7 Pa (500 mtorr) and (a) 10 sccm, (b) 18 sccm, and (c) 100 sccm. PLIF images (d)–(f) show the effect of varying pressure on the CF_2 density in 75% CF_4/Ar discharges at 12 W, 10 sccm, and (d) 13.3 Pa (100 mtorr), (e) 33.3 Pa (250 mtorr), and (f) 133.3 Pa (1000 mtorr). (a)–(e) have been scaled as indicated to highlight the CF_2 distribution, but all are shown on the same relative scale of 0–255 counts.

rate primarily depends on the CF_2 (and F) concentration. The decrease in $[CF_2]$ at low flowrates is therefore attributed to increased losses by diffusion, either by surface losses or by transport out of the imaged region. This increase in diffusional losses may result from an increase in the neutral gas temperature and, hence, diffusion coefficient (note that diffusion coefficient $\propto T^{3/2}$). An increase in the temperature is expected as the flowrate is reduced, because with a constant RF power and a reduced enthalpy efflux, more thermal energy accumulates within the discharge. Such an increase in the contribution of diffusion and surface recombination reactions at low flowrates has been indicated in a previous modeling of F-atom concentration in CF_4/O_2 plasmas [5].

Increasing the pressure at constant power and flowrate [Fig. 1(d)–(f)] leads to increased CF_2 density and rather dramatic changes in its distribution. These changes are due to a complex interaction among the high energy electron impact production and the various transport and loss mechanisms of CF_2. While axial ($r = 0$) argon emission profiles suggest that the CF_2 production profile changes from a peaked asymmetric to a fairly uniform profile as the pressure is increased from 13.3 to 133.3 Pa, the relative roles of diffusion, gas-phase recombination, and convective losses are not as obvious. Due to these complexities, the understanding of these observed pressure-dependent CF_2 distributions would clearly benefit from detailed modeling studies.

References

[1] B. K. McMillin and M. R. Zachariah, "Two-dimensional laser-induced fluorescence imaging of metastable density in low-pressure RF argon plasmas with added O_2, Cl_2 and CF_4," *J. Appl. Phys.*, and references therein, vol. 79, pp. 77–85, 1996.

[2] *Plasma Etching—An Introduction*, D. M. Manos and D. L. Flamm, Eds. Boston: Academic, 1989.

[3] B. K. McMillin and M. R. Zachariah, "2-D imaging of CF_2 density by laser-induced fluorescence of CF_4 etching plasmas in the GEC RF reference cell," in *Proc. 12th Int. Symp. Plasma Chem.*, Minneapolis, MN, Aug. 21–25, 1995, pp. 539–544.

[4] D. B. Oh, A. C. Stanton, H. M. Anderson, and M. P. Splichal, "*In situ* diode laser absorption measurements of plasma species in a GEC reference cell reactor," *J. Vacuum Sci. Technol. B*, vol. 13, pp. 954–961, 1995.

[5] M. Dalvie and K. F. Jensen, "The importance of free radical recombination reactions in CF_4/O_2 plasma etching of silicon," *J. Vacuum Sci. Technol. A*, vol. 8, pp. 1648–1653, 1990.